



#### **OPEN ACCESS**

EDITED BY Hang Lv,

China University of Petroleum Beijing, Karamay Campus, China

REVIEWED BY

Xin Wang,

Chengdu University of Technology, China Dabin Guo,

Guangzhou University, China

Xinquan Zhou, Huanghe Sanmenxia Hospital

Huanghe Sanmenxia Hospital Affiliated to Henan University of Science and Technology, China

\*CORRESPONDENCE

Hongyan Li

☑ lihongyan@ccit.edu.cn

RECEIVED 15 May 2025 ACCEPTED 29 August 2025 PUBLISHED 02 October 2025

#### CITATION

Li H, He Y, Long B, Li X, Tian X, Li S and Ma L (2025) Struvite as a sustainable fertilizer: nutrient recovery from corn starch wastewater with minimal sludge production. *Front. Water* 7:1629179. doi: 10.3389/frwa.2025.1629179

#### COPYRIGHT

© 2025 Li, He, Long, Li, Tian, Li and Ma. This is an open-access article distributed under the terms of the Creative Commons Attribution License (CC BY). The use, distribution or reproduction in other forums is permitted, provided the original author(s) and the copyright owner(s) are credited and that the original publication in this journal is cited, in accordance with accepted academic practice. No use, distribution or reproduction is permitted which does not comply with these terms.

# Struvite as a sustainable fertilizer: nutrient recovery from corn starch wastewater with minimal sludge production

Hongyan Li<sup>1,2\*</sup>, Yong He<sup>1,3</sup>, Beisheng Long<sup>4</sup>, Xiaodan Li<sup>5</sup>, Xi Tian<sup>1,2</sup>, Songsong Li<sup>1</sup> and Li Ma<sup>1</sup>

<sup>1</sup>School of Municipal and Environmental Engineering, Changchun Institute of Technology, Changchun, China, <sup>2</sup>Jilin Provincial Key Laboratory of Municipal Wastewater Treatment, Changchun Institute of Technology, Changchun, China, <sup>3</sup>China Construction Xinjiang Construction Engineering Group Third Construction Engineering Co., Ltd., Urumqi, China, <sup>4</sup>School of Energy and Environmental Engineering, Jilin University of Architecture and Technology, Changchun, China, <sup>5</sup>China Northeast Municipal Engineering Design and Research Institute Co., Ltd., Changchun, China

**Introduction:** The deep-processing corn industry produces nutrient-rich wastewater that exacerbates eutrophication in water bodies, necessitating the development of sustainable nutrient-recovery methods.

**Methods:** This study introduces a sensor-integrated struvite crystallization method for nitrogen (N) and phosphorus (P) recovery from cornstarch wastewater through struvite crystallization.

**Results:** Using real-time pH and ion sensors, the conditions were optimized (pH 10.50, Mg/P ratio 2.0, 30°C, 35 min, 180 rpm), which recovered 98.52% of P and high N rates. Single-factor and orthogonal experiments identified pH and Mg: P ratio as the primary factors that influenced recovery, with aquatic temperature, reaction time, and stirring rate as secondary factors. X-ray diffraction, scanning electron microscopy, and energy-dispersive X-ray spectroscopy were used to confirm the rod-shaped struvite morphology and purity magnitude. Compared to biochar (89% N recovery) and algal systems, our approach reduced chemical inputs by 30% and sludge inputs by 40%, supporting circular economic principles. Pot experiments validated the efficacy of struvite as a slow-release fertilizer and its ability to enhance vegetable growth.

**Discussion:** This sensor-driven method offers an innovative and eco-friendly solution for managing agro-industrial wastewater.

**Conclusion:** This mitigates eutrophication and promotes resource recovery in the corn-processing industry.

KEYWORDS

struvite crystallization, nutrient recovery, corn starch wastewater, eutrophication mitigation, sensor-based monitoring

#### Introduction

The corn deep-processing industry plays a vital role in the economies of many countries by producing starch, sweeteners, and biofuels. However, it generates substantial amounts of wastewater enriched with unused nitrogen (N) and phosphorus (P) (Sajjad et al., 2024). If not effectively treated, nutrient release can trigger eutrophication in natural drainage basins, a process caused by excessive nutrient enrichment that leads to algal blooms and oxygen depletion in water bodies (Adetunji et al., 2023). For example, untreated effluent from corn starch facilities in the Midwestern United States has been identified as a precondition for severe eutrophication in the Mississippi River Basin,

contributing to the Gulf of Mexico's hypoxic 'dead' zone (The Nature Conservacy, 2025). In China, poorly managed wastewater from corn processing plants along the Yellow River has been reported to cause nutrient overload, persistent algal blooms, and ecological degradation (Zhu et al., 2020). To address this challenge, innovative strategies are required to recover and recycle nutrients from corn industry wastewater with the expected purpose to reduce threats to the basin environment.

Recent studies have highlighted the potential of agricultural waste-derived materials to capture N and P for reuse in crop production (Bermúdez et al., 2024; Rekaby et al., 2021). For example, biochar produced from corncobs or straw can enhance aqueous P adsorption by magnesium oxide nanoparticles (Zhou et al., 2024; Zhu et al., 2020). Similarly, algal systems can recover nutrients from dairy waste streams, suggesting their applicability in corn wastewater (Luzzi et al., 2024; Mohsenpour et al., 2021). These approaches align with circular economy principles that advocate the transformation of waste components into resources (Vunnava and Singh, 2021). The integration of technologies for optimizing organic loading rates can further enhance the nutrient recycling efficiency (Aamir and Hassan, 2025; Wan et al., 2023). The corn industry can mitigate eutrophication risks by leveraging these advancements to support sustainable agriculture (Fendel et al., 2022). It is necessary to explore the feasibility and efficacy of such waste-derived solutions and to draw on recent research to propose pathways for nutrient management.

Wastewater generated by the corn starch deep-processing industry is characterized by high ammonium nitrogen (N) (>260 mg/L), high total phosphorus (P) (>60 mg/L), and a low carbonto-nitrogen (C/N) ratio (<1.5) (Chamas et al., 2020; Zhai et al., 2022; Zhang et al., 2022). Current nutrient removal methods exhibit notable drawbacks because of the extensive use of Premoval chemicals, which leads to the production of N- and P-rich chemical sludges and increases the risk of secondary environmental contaminants (Mohan et al., 2020; Zhang B. et al., 2023). Poor performance stems from excessive reliance on chemical precipitation, which fails to address low C/N ratios and hinders biological nutrient removal (Zhang D. et al., 2023). It has been suggested that recovering N and P using wastederived materials can significantly reduce residuals while recycling nutrients (Lessmann et al., 2023; Sniatała et al., 2024; Tarigan et al., 2025). These approaches are currently supported by the use of biochar and algal systems, which offer sustainable pathways for pollution mitigation and resource conservation (Rickard, 2023; Strawn et al., 2023). However, the effectiveness of nutrient absorption by these biotic systems may be influenced by multiple pre- and postprocessing treatments. Furthermore, the use of biochar may pose additional risks in terms of adsorption variability, potential contamination, and N collection (Dong et al., 2023; Nobaharan et al., 2021; Zheng et al., 2018). The utilization of algae may also be associated with high harvesting costs, pathogen and toxin infections, and stringent land requirements (CDC, 2024; Kim et al., 2018; Yaakob et al., 2021). Therefore, abiotic approaches are more suitable for removing high N and P concentrations from wastewater residuals, with reactions fully monitored by sensors in a synthesized system.

Struvite crystallization is known as magnesium ammonium phosphate (MgNH<sub>4</sub>PO<sub>4</sub>·6H<sub>2</sub>O). Struvite precipitation is a

promising method for nutrient recovery. It offers a sustainable alternative to abiotic N–N–N-P-removers with a stable effectiveness. This process occurs when the concentrations of Mg<sup>2</sup>+, PO<sub>4</sub><sup>3-</sup>, and NH<sub>4</sub><sup>+</sup> in wastewater exceed the solubility product constant (Ksp; the critical value of  $2.5 \times 10^{-13}$ ). This was reported to further precipitate NH<sub>4</sub><sup>+</sup> and PO<sub>4</sub><sup>3-</sup> as struvite crystals via the following reaction (Aka et al., 2024):

$$Mg^{2+} + PO_4^{3-} + NH_4^+ + 6H_2O \rightarrow MgNH_4PO_4 \cdot 6H_2O \downarrow$$
 (1)

This can result in the reduction of residuals of N and P in wastewater and mitigation of the environmental burden while recovering nutrients for potential reuse (Tarigan et al., 2025). Struvite crystallization in cornstarch wastewater curbs the high demand for chemicals and energy in conventional treatments. This can address alkali consumption by reducing the need for external alkali addition to adjust the pH, which can further decrease the amount of sludge generated through the recovery of valuable nutrients (Geng et al., 2024). However, its efficacy hinges on controlling the key process facets of the solution pH, molar ratios, and reaction conditions, which must be optimized collectively to ensure the maximization of success (He et al., 2022). Studies have confirmed its potential to alleviate eutrophication by reducing P discharge (Wang et al., 2023); however, its implementation requires precise management to ensure consistent outcomes (Oliveira et al., 2021; Pesonen et al., 2020).

The conditions that determine the efficacy of N and P extracts using struvite include the optimum pH, molar ratio of Mg to P, aquatic temperature, reaction time, and stirring rate (Mugwili et al., 2023; Saidou et al., 2009; Santos et al., 2024). The pH value that governs struvite solubility and precipitation efficiency is typically optimal [approximately 9.5 (Aguilar-Pozo et al., 2023)]. The Mg to P molar ratio is often maintained above 1:1, which ensures sufficient magnesium availability for crystal formation (Patel et al., 2023). The ideal water temperature for the reaction with struvite is ideally-25-30°C, as it was suggested to accelerate the reaction kinetics and enhance the struvite yield (Qi et al., 2024). The reaction time can range from minutes to hours, with a longer reaction time resulting in greater nutrient removal (Li et al., 2019; Liu et al., 2011). The reaction is promoted by the stirring rate; however, an adequate stirring rate facilitates homogeneous mixing and crystal growth (Jaramillo et al., 2018). These facets collectively dictate the process efficiency, and it is necessary to precisely control their co-effects using sensors for optimal overall performance.

Monitoring the reaction conditions using sensors is pivotal for real-time process optimization. The pH sensors detect shifts critical for ammonia stripping and P precipitation, as demonstrated using hollow fiber membrane contactors (Noriega-Hevia et al., 2023). Conductivity sensors correlate ion variations with P uptake in sequencing batch reactors (Aguado et al., 2006; Kim et al., 2007). Temperature sensors ensure optimal reaction conditions, whereas oxygen uptake rate measurements adjust aeration duration to enhance nitrification (How et al., 2019; Shourjeh et al., 2020). Oxidation–reduction potential (ORP) sensors identify denitrification endpoints that can be used to optimize anoxic phases (Casellas et al., 2006). Such sensor-based control improves N and P removal efficiencies, reduces energy costs, and adapts to influent variability (Romero et al., 2023). Despite these advances,

the synthesis of sensors for the simultaneous monitoring and control of all facets remains scarce, owing to the limited number of studies integrating multifaceted sensor systems (Siontorou et al., 2017). Although the development of such technologies is essential for comprehensive process management, research gaps persist, underscoring the need for innovative sensor design (Alatawi et al., 2025; Petrea et al., 2023).

In this study, we conducted an evidence-based study to verify the reaction performance of the N and P recycling rates from cornstarch wastewater using a self-manufactured facility with multiple sensors. The objectives of this study were to (1) optimize the recovery of nitrogen and phosphorus from cornstarch wastewater using struvite precipitation and (2) evaluate the purity and morphological characteristics of the recovered product. Single-factor and orthogonal experimental designs were used to identify key factors and determine the optimal levels of N and P recovery. This approach aims to enhance the recovery efficiency while simultaneously minimizing treatment costs and environmental impacts. The main components, crystal morphology, and purity of the recovered product were analyzed using X-ray diffraction (XRD), scanning electron microscopy (SEM), and energy-dispersive spectroscopy (EDS) to verify its potential as a recycled fertilizer. In addition, we propose three hypotheses. First, the recovery efficiency of nitrogen and phosphorus from corn starch wastewater using the struvite crystallization method was significantly influenced by the pH, water temperature, molar ratio of Mg<sup>2+</sup> to P, reaction time, and stirring rate. Second, the optimal conditions for N and phosphorus recovery from cornstarch wastewater using struvite crystallization can achieve high recovery rates of PO<sub>4</sub><sup>3-</sup>-P and NH<sub>4</sub><sup>+</sup>-N, with the recovered product being predominantly high-purity struvite. Finally, struvite has the potential to be utilized as a slow-release fertilizer owing to its composition, morphology, and purity.

#### Materials and methods

#### Wastewater materials

Effluent water quality was analyzed using the internal circulation (IC) anaerobic reactor of a wastewater treatment plant owned by a large cornstarch enterprise. Pre-investigation results indicated that the chemical oxygen demand measured using potassium dichromate (K<sub>2</sub>Cr<sub>2</sub>O3) (CODCr) ranged from 210 to 560 mg·L¹, NH<sub>4</sub><sup>+</sup>-N ranged from 260 to 380 mg·L¹, PO<sub>4</sub><sup>3-</sup>-P ranged from 60 to 90 mg·L¹, and pH fluctuated between 7.28 and 7.52. Based on these values, simulated wastewater was prepared by dissolving soluble starch, NH 3 Cl solution, KH<sub>2</sub>PO 3 solution, and tap water. The specific composition of the simulated wastewater was  $\rho(\text{CODCr})$  of 300 mg L $^{-1}$ ,  $\rho(\text{NH}_4^+\text{-N})$  of 300 mg L $^{-1}$ ,  $\rho(\text{PO}_4^{3-}\text{-P})$  of 80 mg L $^{-1}$ , and pH values 6.56 of 6.82.

## **Experimental materials**

The chemical reagents used in this study included magnesium oxide (MgO), magnesium chloride (MgCl<sub>2</sub>·6H<sub>2</sub>O), potassium

hydrogen phosphate ( $KH_2PO_4$ ), ammonium chloride ( $NH_4Cl$ ), sodium hydroxide (NaOH), and hydrochloric acid (HCl). All the chemicals were of analytical grade and were not subjected to further purification.

## **Experiment layout**

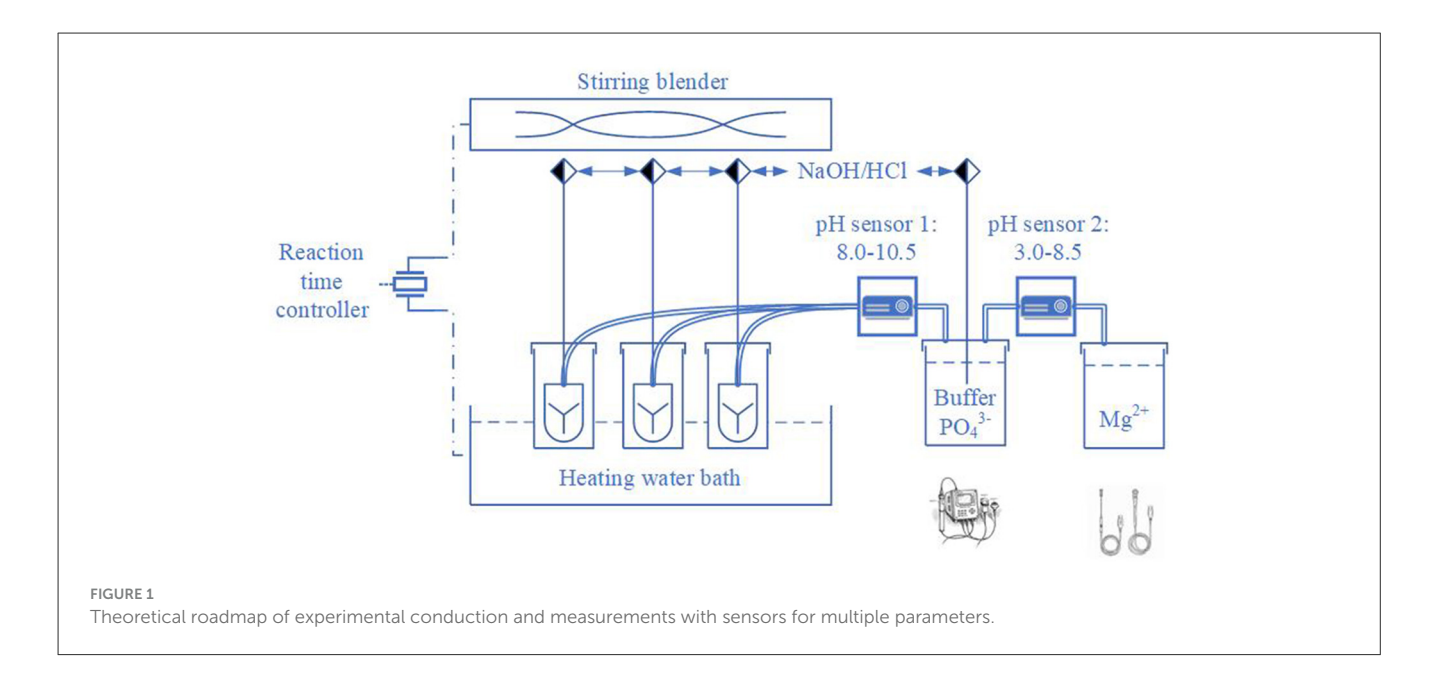
#### Experimental layout and sensors placement

The experiment was conducted under controlled conditions in a facility using an integrated sensor. The framework was supported by a water bathing tank equipped with aquatic sensors to maintain constant aquatic temperatures (HH-8, Kexi Instrument Inc., Jintan, China). It was framed using a stirring blender skeleton, which was pillared by a panel with three stirring rods (JJ-4A, Kexi Instrument Inc., Jintan, China).

Experimental solutions were prepared in 500 mL aliquots and added to a 1,000 mL beaker. Three beakers were grouped in bulk for testing the main effect conditions in a water bath (Figure 1). The aquatic temperature was monitored using a sensor that switched the water heating to maintain the temperature at the intended level. The electric current for the entire facility was switched using a reaction time controller. Modification of the Mg/P molar ratio was initiated and regulated by adding MgCl<sub>2</sub>·6H<sub>2</sub>O and MgO at a molar ratio of 1:2 to adjust the initial Mg/P molar ratio to 1:1. When the reaction reached the lateral stage, 6 mol L<sup>-1</sup> HCl was added to the solution to stop the reaction by stopping the crystallization. Struvite crystallization was extracted by centrifugation to leave the solution in a beaker for subsequent analyses. One stirring rod was placed in one beaker, where NaOH was added to the solution to adjust the pH value within the range of 8.0-10.5 for the experimental environment, which was monitored by a pH sensor (Sensor 1) equipped over the route of solution flow from beakers to the buffer. The PO<sub>4</sub><sup>3-</sup> anion was measured in this buffer, HCl was added to the buffer to reduce the pH, and NaOH was added when it was excessively acidic. The extracted samples were continuously extracted from the buffer to the Mg<sup>2+</sup> detector only when the pH value fell in the range of 3.0–8.5 by another sensor 2. Before stirring, the sample was extracted from the reaction beaker to the buffer at a flow rate of 1.2 mL  $\ensuremath{\text{s}^{-1}}$  until a total of 15 mL flow went through. The experiment commenced only when the pH value indicated by sensor 1 met the required level and HCl was added to the buffer. The flow continued through sensor 2 at a rate of 1.2 mL s<sup>-1</sup> until a total of 10 mL was added. When the pH of the flow decreased to a range of 3.0-8.5, Mg was monitored using a specific sensor. Subsequently, the molar Mg:P ratio is determined.

#### Ion and anion measures

The  $Mg^{2+}$  solution was monitored using a magnesium ion-selective electrode (ISE) (NTsensor, Vila-Seca, Spain). The sensor measures  $Mg^{2+}$  concentrations ranging from 2.4 to 2,400 mg  $L^{-1}$ , equivalent to  $1\times 10^{-4}$  to 0.1 mol  $L^{-1}$ , with a reproducibility accuracy of  $\pm 20\%$  of the full scale when calibrated between 10 and 1,000 mg  $L^{-1}$ . It is affected by interfering ions, such as  $K^+$  and  $Ca^{2+}$ , and operates effectively within a pH range of 3–8.5 without



pH compensation. The sensor functions at temperatures ranging from  $5^{\circ}C$  to  $50^{\circ}C$  without temperature compensation, exhibits an electrode slope of 24  $\pm$  5 mV, and has an electrode resistance of 1–4  $M\Omega$ . A minimum immersion depth of 2 mm was required, with the body diameter varying depending on the specific sensor model used.

The  $PO_4^{3-}$  anion was detected using an Alyza IQ electrode (Xylem Analytics, YSI Inc., Yellow Springs, OH, USA). The YSI Alyza PO4 analyzer provides precise measurement of phosphate anions across the range from 0.02 to 15.00 mg L $^{-1}$  PO $_4^{3-}$ -P with a displayed range of 0.00 to 15.00 mg L $^{-1}$ , 0.01 mg L $^{-1}$  resolution, and accuracy of  $\pm$  2% or  $\pm$  0.02 mg L $^{-1}$  (whichever is greater) with a displayed range of 0.0 to 50.0 mg L $^{-1}$ , 0.05 mg L $^{-1}$  resolution, and accuracy of  $\pm$  2% or  $\pm$  0.2 mg L $^{-1}$  (whichever is greater). The sampling conditions were maintained at 4–45°C and the pH was controlled from 5 to 9. An optional filtration unit was used for high solids content (up to 6,000 mg L $^{-1}$ ).

Chemical characterization of struvite was performed using a series of experiments. Fourier-Transform Infrared Spectroscopy (FTIR) was performed using a Nicolet iS50 model (Thermo Fisher Scientific, Waltham, MA, USA) to analyze the vibrational modes of NH $_4^+$  (1,400–1,500 cm $^1$ ) and PO $_4^{3-}$  (900–1,100 cm $^1$ ) in struvite crystals (Kowalczuk and Pitucha, 2019). X-ray photoelectron spectroscopy (XPS) (K-Alpha, Thermo Fisher Scientific) was used to determine the surface elemental composition and oxidation states of Mg, P, and N (Woodruff, 2016). The EDS settings (e.g., 5–20 kV,  $\sim$ 130 eV resolution) were specified, and the elemental ratios (Mg: P: N) were quantified to validate the stoichiometry of struvite (Sidorczuk et al., 2020).

#### Single factor experiment

Simulated wastewater (500 mL) was collected and placed in a 1,000 mL beaker. According to the initial molar ratio of  $NH_4^+-N$  to  $PO_4^{3-}-P$  in the simulated wastewater (8.3), the  $NH_4^+-N$  content

was excessive compared to the ordinary levels. Therefore, during the experiment, MgO and MgCl<sub>2</sub>·6H<sub>2</sub>O were added to the reactive solution based on the PO<sub>4</sub><sup>3-</sup>-P content (with the molar ratio of MgCl<sub>2</sub>·6H<sub>2</sub>O to MgO fixed at 1:2). Single-factor experiments were conducted under different conditions with varying pH, Mg/P molar ratio, aquatic temperature, reaction time, and stirring rate. In detail, pH was set in values of 8.00, 8.50, 9.00, 9.50, 10.00, 10.50; the molar ratio of Mg/P in 1.0, 1.2, 1.4, 1.6, 1.8, and 2.0; aquatic temperature was set to be  $5^{\circ}$ C,  $10^{\circ}$ C,  $15^{\circ}$ C,  $20^{\circ}$ C,  $25^{\circ}$ C,  $30^{\circ}$ C,  $35^{\circ}$ C, and  $40^{\circ}$ C; reaction time was set to be 5 min, 10 min, 20 min, 30 min, 35 min, 40 min, 50 min, and 60 min; stirring rate was set to be 50 r⋅min<sup>1</sup>, 80 r·min<sup>1</sup>, 100 r·min<sup>1</sup>, 120 r·min<sup>1</sup>, 150 r·min<sup>1</sup>, 180 r·min<sup>1</sup>, and 210 r·min<sup>1</sup>. Immediately after the reaction, 6 mol·L<sup>1</sup> HCl was added to the wastewater sample and the mixture was centrifuged. The concentrations of  $NH_4^+$ -N and  $PO_4^{3-}$ -P were measured in the filtrate, and the recovery rates of  $NH_4^+$ -N and  $PO_4^{3-}$ -P were calculated. The main effects of different pH values, molar ratio of Mg/P, aquatic temperature, reaction time, and stirring rate were analyzed on the recovery efficiencies of  $NH_4^+$ -N and  $PO_4^{3-}$ -P.

Single-factor experiments were performed under specified experimental conditions. A volume of 500 mL of cornstarch wastewater was used as a simulation (CODCr: 300 mg/L, NH<sub>4</sub><sup>+</sup>-N: 300 mg/L, PO<sub>4</sub><sup>3</sup>-P: 80 mg/L, pH 6.56-6.82) in 1,000 mL beakers. MgO and MgCl<sub>2</sub>·6H<sub>2</sub>O (molar ratio 2:1) were added based on the PO<sub>4</sub><sup>3</sup>-P. One factor varied per test in pH of 8.0-10.5, Mg/P molar ratio of 1.0-2.0, aquatic temperature of 5-40°C, reaction time of 5-60 min, and stirring rate of 50-210 rpm. In the post-reaction, a volume of 6 mol/L HCl was added to stop crystallization; thereafter, the samples were centrifuged, and NH<sub>4</sub><sup>+</sup>-N/PO<sub>4</sub><sup>3</sup>-P recovery rates were calculated.

#### Orthogonal experiment

The single-factor experiment preliminarily optimized the factors affecting struvite crystal precipitation but did not identify

the optimal combination of conditions for struvite precipitation. Based on the single-factor experiment results, the pH value (A), Mg/P molar ratio (B), aquatic temperature (C), stirring rate (D), and reaction time (E) were selected as factors, with the recovery rates of NH<sub>4</sub><sup>+</sup>-N and PO<sub>4</sub><sup>3-</sup>-P as the response variables for the orthogonal experiment. An L16(45) orthogonal experiment was designed (Table 1) targeting the range of values around the single-factor optimization results, and a range analysis was used to determine the significance of the effects of the factors on the yield. Range analysis is a method for analyzing orthogonal experimental results, where factors with a larger range (R) have a greater impact on recovery rates, whereas factors with a smaller range suggest lower significance. Range R is the difference between the maximum and minimum average values of the levels, with K1i and K2i representing the average recovery rates for level i of each factor column in Table 1.

## Post-crystallization analysis

Immediately after the experiment, 6 mol·L¹ hydrochloric acid was added to the water sample to stop the crystallization reaction. The sample was centrifuged to separate the supernatant, which was then retained for analysis. The precipitated crystals were filtered through a 0.45  $\mu m$  membrane, dried at 40°C for 48 h, and used for subsequent purity determination, as well as component and morphological analysis of the recovered product.

Ammonia-N was measured using Nessler's reagent photometric method. The sample was pretreated with sodium thiosulfate to eliminate any interference such as chlorine. If necessary, flocculent precipitation was performed using zinc sulfate and NaOH followed by filtration of the supernatant. For color development, alkaline Nessler's reagent (potassium tetraiodomercurate (II) in NaOH) was added to the sample and reacted with ammonia to form a yellowish-brown colloidal complex. Potassium sodium tartrate was added as a stabilizer and the absorbance of the colored solution was measured using a spectrophotometer at approximately 420-430 nm. The phosphate concentration was determined using the molybdenum-antimony anti-spectrophotometric method. The recovered product was analyzed using X-ray diffraction (XRD) and scanning electron microscopy with energy-dispersive X-ray spectroscopy (SEM-EDX-EDS). XRD was performed using Cu-Kα radiation ( $\lambda = 1.5406 \text{ Å}$ ) to analyze the crystallographic structure and determine the phase composition, lattice parameters (e.g., a = 3.5-10 Å), and crystallite sizes (typically 10-100 nm) by measuring the diffraction angles ( $2\theta = 10-80^{\circ}$ ). SEM with energydispersive X-ray spectroscopy (EDS) provided morphological and elemental insights during operation at 5-20 kV, resulting in the generation of high-resolution images. Visible results can be magnified up to 100,000 × until they reveal the surface features of an apparent quality (e.g., 10 nm resolution). EDS has an energy resolution of ~130 eV and can be used to identify the elemental compositions (e.g., C, O, and Fe) and quantify their weight percentages.

#### Variable calculation and statistics

As struvite is the only crystalline substance that contains N (magnesium ammonium phosphate, MgNH4PO4·6H<sub>2</sub>O, abbreviated as MAP), the purity of struvite can be characterized by its N content, according to the following formula:

$$\mu_{MAP} = \frac{n_N \times M_{MAP}}{m_c} \times 100\% \tag{2}$$

where  $\mu_{MAP}$  is the percentage of struvite purity,  $n_N$  is the molar amount of N component in struvite,  $M_{MAP}$  is the molar amount of struvite, and  $m_c$  is the mass quality of the recovery. In addition, the recovery rates  $(\eta)$  of NH<sub>4</sub><sup>+</sup>-N and PO<sub>4</sub><sup>3-</sup>-P were calculated as follows:

$$\eta = \frac{(C_0 - C_e)}{C_0} \times 100\% \tag{3}$$

where  $C_0$  is the initial concentration of either NH<sub>4</sub><sup>+</sup>-N or PO<sub>4</sub><sup>3-</sup>-P (mg L<sup>-1</sup>) and  $C_e$  is the concentration in the post-recycling wastewater (mg L<sup>-1</sup>).

SAS software (9.4 version, SAS Statistics Inc., Cary, NC, USA) was used for statistical analysis. In the single-factor experiment, the results were compared using one-way analysis of variance (ANOVA), and the results were calculated as means and standard errors. The condition-response records were fitted using the curves derived from the highest determinant coefficient. The XRD pattern of the struvite precipitate was analyzed using the Jade 6.5 software (Materials Data Inc., Livermore, CA, USA), and the XRD spectra were plotted with data derived from either standard references or struvite objectives. In SAS, the PROC FACTEX was used to generate orthogonal fractional factorial designs, and the PROC GLM was employed to analyze the results of the orthogonal model.

## Results

#### Single-factor experiment results

#### pH value gradient

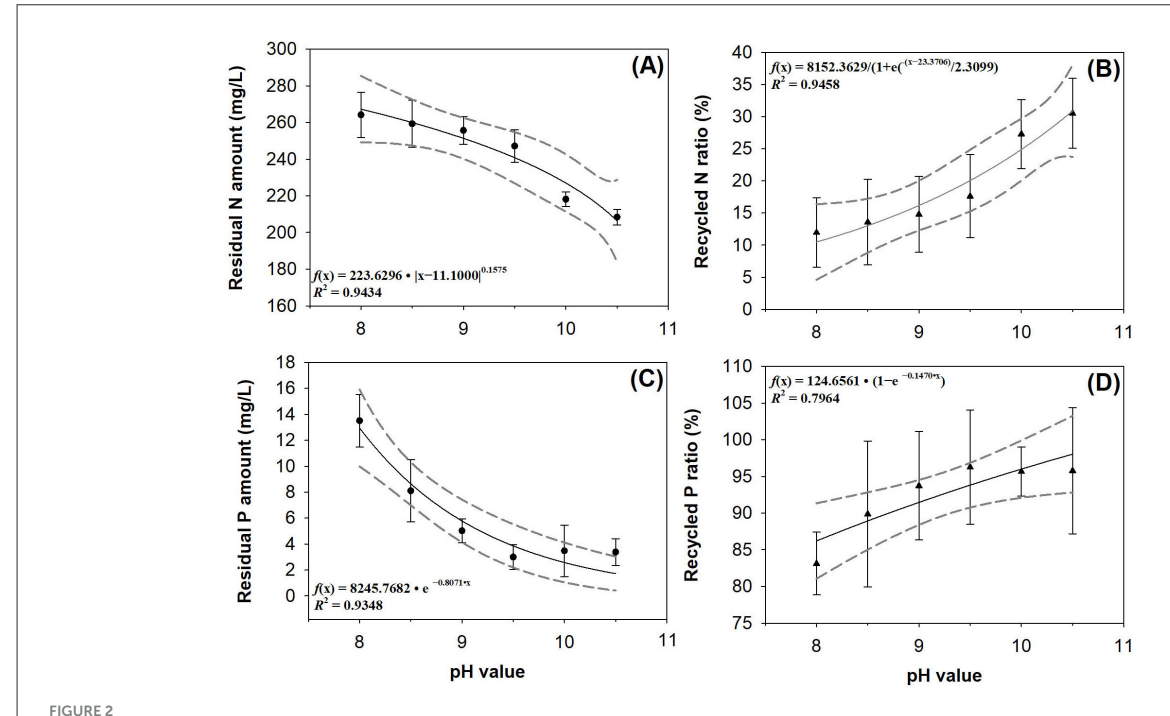
The responses of the residual N amount to pH values can be curved by a symmetric power equation, which indicates that the pH value was infinitely close to 11.10 to minimize the residual N amount (Figure 2A). The recycled N ratio responded to the pH values that could be fitted to the curve of a sigmoidal exponential function (Figure 2B). Therefore, the midpoint that marks the inflection was 23.37, which is against a reasonable situation; hence, the pH value increased at a steepness lower than 2.31. The amount of residual P responded to the pH values that could be fitted to an exponential decay curve, which resulted in a decay rate of 0.8071 (Figure 2C). The response of the recycled P ratio to the pH value can be fitted using the rise-to-maximum exponential function, which indicates that the recycled P ratio reached a maximum ratio of 100% when the pH value was 11.05 (Figure 2D).

#### Mg/P molar ratio

The residual N amount responded to the increase in the Mg/P molar ratio, which could be fitted by an exponential decay

TABLE 1 Factors and levels of orthogonal experiments for recovery process optimization.

Level	Factors							
	pH (A)	Mg/P molar ratio (B)	Aquatic temperature (°C)/(C)	Stirring rate (r $\min^{-1}$ )/(D)	Reaction time (min)/(E)			
1	9.00	1.4	15	100	20			
2	9.50	1.6	20	120	30			
3	10.00	1.8	25	150	35			
4	10.50	2.0	30	180	40			



Amounts and recycled ratios of nitrogen (N) and phosphorus (P) in post-experiment residuals (A, C) over the process where N and P were recycled (B, D) in response to the pH gradient. Plots mark means with boxes being representative for N and triangles for P. Error bars represent standard errors. The full lines mark the fit curves, with dashed lines framing the 95% confidence bands. In cell D, the maximum of y-axis is capped to 100% to prevent error overflow to the biased range over 100%.

curve, with a decay rate of 0.0214 (Figure 3A). The response of the recycled N ratio to the Mg/P molar ratio was fitted by an increase-to-maximum exponential curve, which had an increasing rate of 2.90 with a theoretical maximum of 29.23% (Figure 3B). The amount of residual P responded to the Mg/P molar ratios that could be fitted by an exponential decay curve, which resulted in a decay rate of 1.5415 (Figure 3C). The response of the recycled P to the Mg/P molar ratio can be fitted by the rise-to-maximum exponential function, which indicates that the recycled P ratio reached a maximum ratio of 98.52% at an increasing Mg/P ratio of 3.00 (Figure 3D).

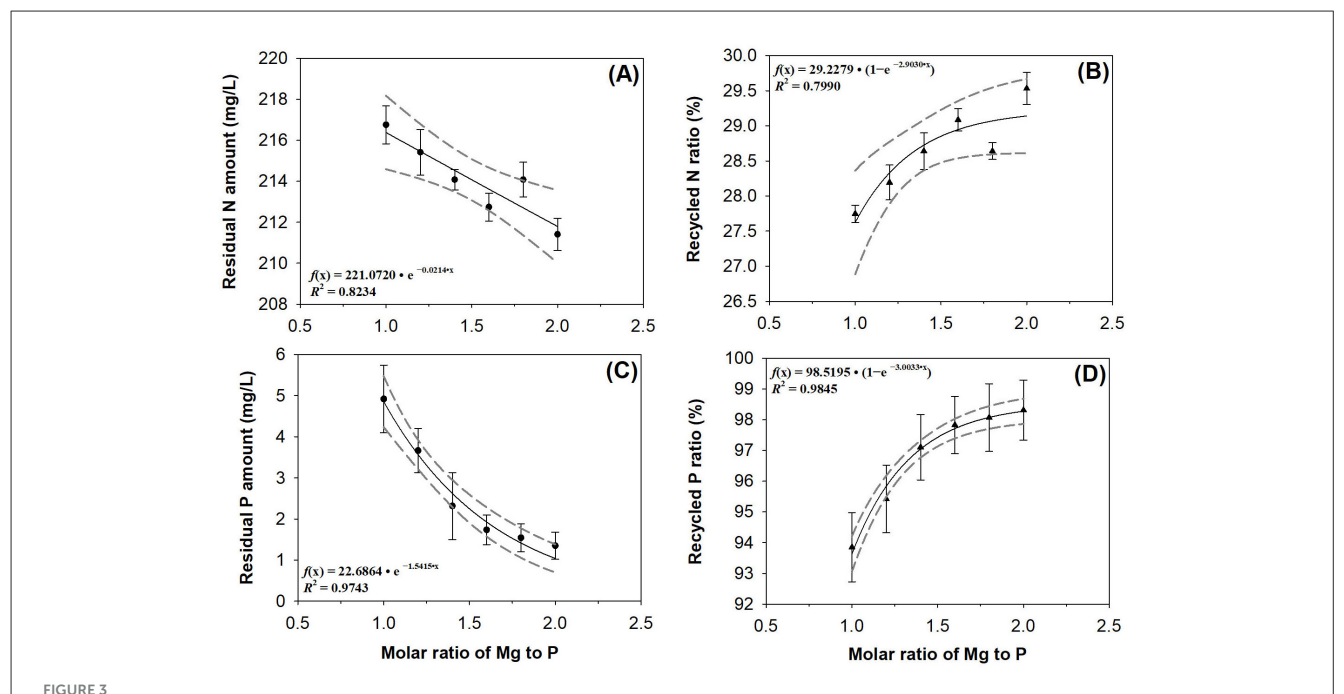
## Aquatic temperature

The response of the amount of residual N to aquatic temperature can be fitted by a 3-parameter symmetric power curve (Figure 4A). Therefore, the residual N amount can be 265.8 mg  $\rm L^{-1}$  at an initial aquatic temperature of 5°C, and the residual N

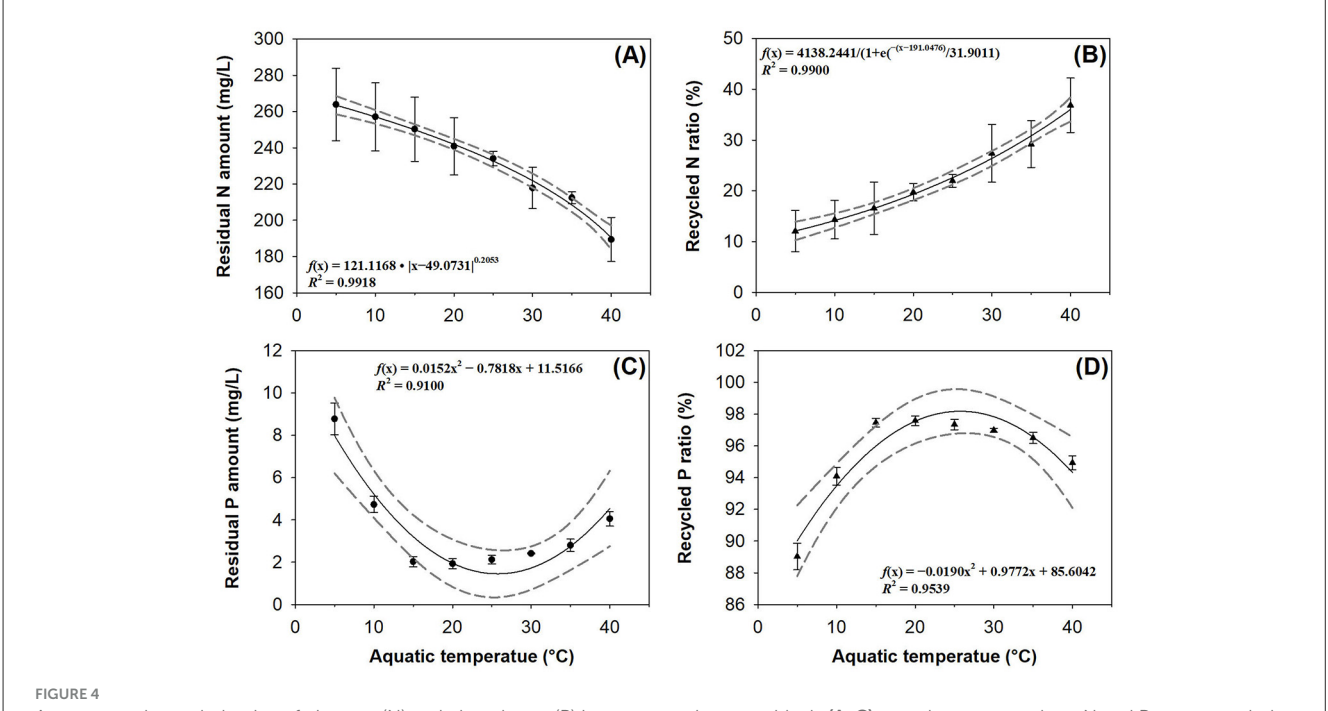
amount would reach zero if the aquatic temperature was  $49.0731^{\circ}$ C. The responses of recycled N ratio can be fitted by a curve of sigmoid function, where the midpoint was  $191.05^{\circ}$ C which was much higher than the highest reasonable temperature of  $40^{\circ}$ C, and the steepness was lower than 31.90 (Figure 4B). The response of the residual P amount to aquatic temperature can be fitted by a quadratic polynomial curve, which indicated a minimum P amount of  $1.49\,\mathrm{mg}$  L $^{-1}$  when the aquatic temperature was  $25.72^{\circ}$ C (Figure 4C). The response of the recycled P ratio to aquatic temperature can also be fitted by a quadratic polynomial curve, which indicated a maximum recycled P ratio of 98.12% when the aquatic temperature was  $25.72^{\circ}$ C (Figure 4D).

#### Reaction time

The response of the amount of residual N to the reaction time can be fitted by an exponential decay curve, which results in a decay rate of 0.0048 (Figure 5A). The recycled N ratio increased



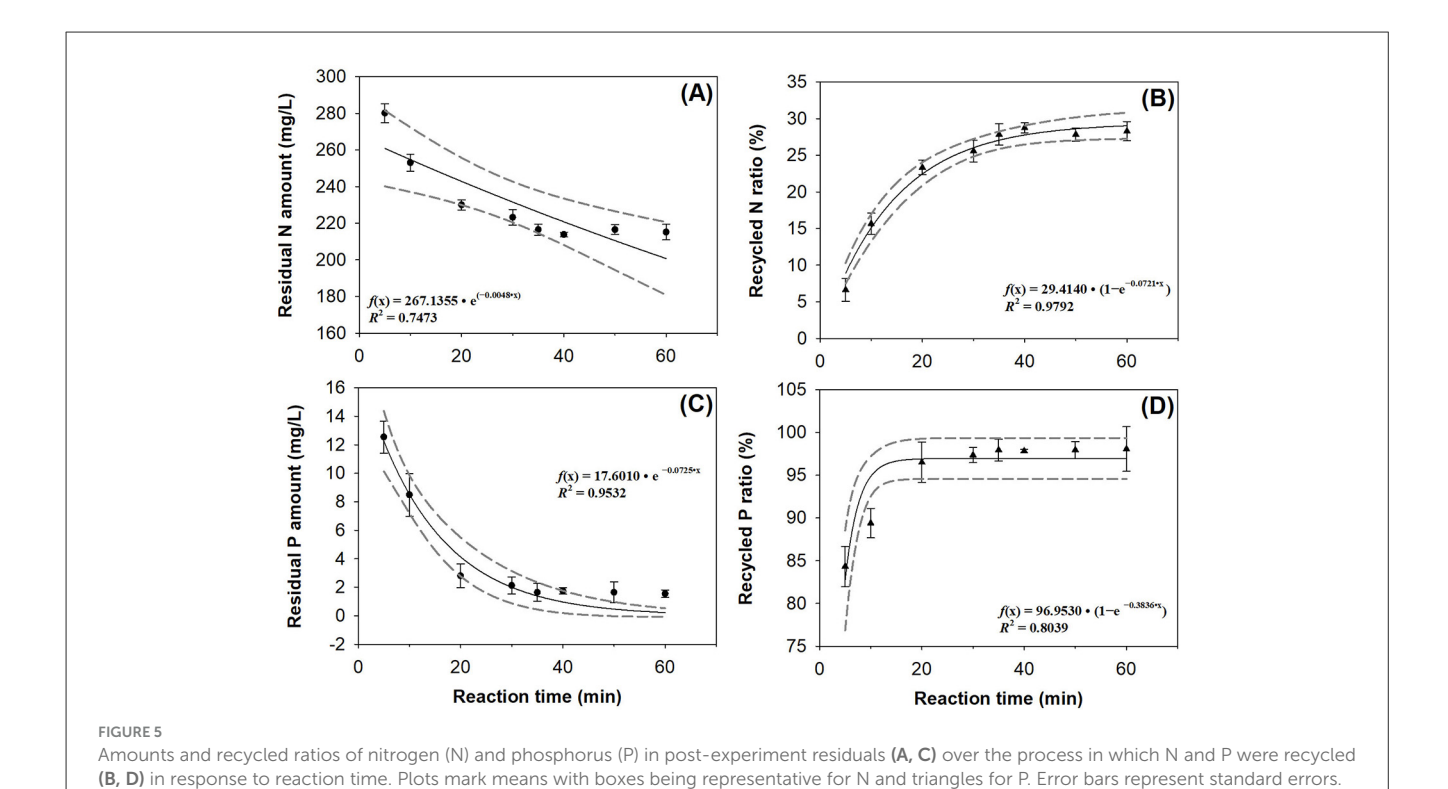
Amounts and recycled ratios of nitrogen (N) and phosphorus (P) in post-experiment residuals (A, C) over the process in which N and P were recycled (B, D) in response to Mg/P molar ratios. Plots mark means with boxes being representative for N and triangles for P. Error bars represent standard errors. The full lines mark the fit curves, with dashed lines framing the 95% confidence bands.



Amounts and recycled ratios of nitrogen (N) and phosphorus (P) in post-experiment residuals (A, C) over the process where N and P were recycled (B, D) in response to aquatic temperature. Plots mark means with boxes being representative for N and triangles for P. Error bars represent standard errors. The full lines mark the fit curves, with dashed lines framing the 95% confidence bands.

with the reaction time, which can be fitted by a rise-to-maximum exponential curve, indicating that the maximum recycled N ratio was 29.41% at an increasing rate of 0.07 (Figure 5B). In contrast,

the amount of residual P decreased with reaction time, which could be fitted by an exponential decay curve at a decreasing rate of 0.07 (Figure 5C). Theoretically, the recycled P ratio was maximized at



96.95% when the reaction time was infinitely increased (Figure 5D). When the reaction time reached a maximum level of 60 min, the recycled P ratio was 96.95%.

The full lines mark the fit curves, with dashed lines framing the 95% confidence bands

## Stirring rate

The amount of residual N decreased with increasing stirring rate, which could be fitted by an exponential decay curve at a decreasing rate of 0.0011 (Figure 6A). In contrast, the recycled N ratio increased with increasing stirring rate to a maximum level of 31.93% (Figure 6B). Again, the residual P amount also decreased with stirring rate, which was fitted by an exponential decay curve at a decline rate of 0.02 (Figure 6C). The recycled P ratio increased with increasing stirring rate to a maximum level of 97.84% (Figure 6D).

#### Orthogonal experiment results

The performance of a 5-factor and 4-level orthogonal experiment yielded the results listed in Table 2. R1 values decreased in the following order: pH > aquatic temperature > reaction time > stirring rate > Mg/P molar ratio. Accordingly, the order of significance of the factors affecting the NH<sup>4+</sup>-N recovery rate in the simulated wastewater was pH > aquatic temperature > reaction time > stirring rate > Mg/P molar ratio. Therefore, the main factors that influenced the NH<sup>4+</sup>-N recovery rate were pH and aquatic temperature, whereas the secondary factors were reaction time, stirring rate, and Mg/P molar ratio. According to the orthogonal experimental results for the average NH<sup>4+</sup>-N

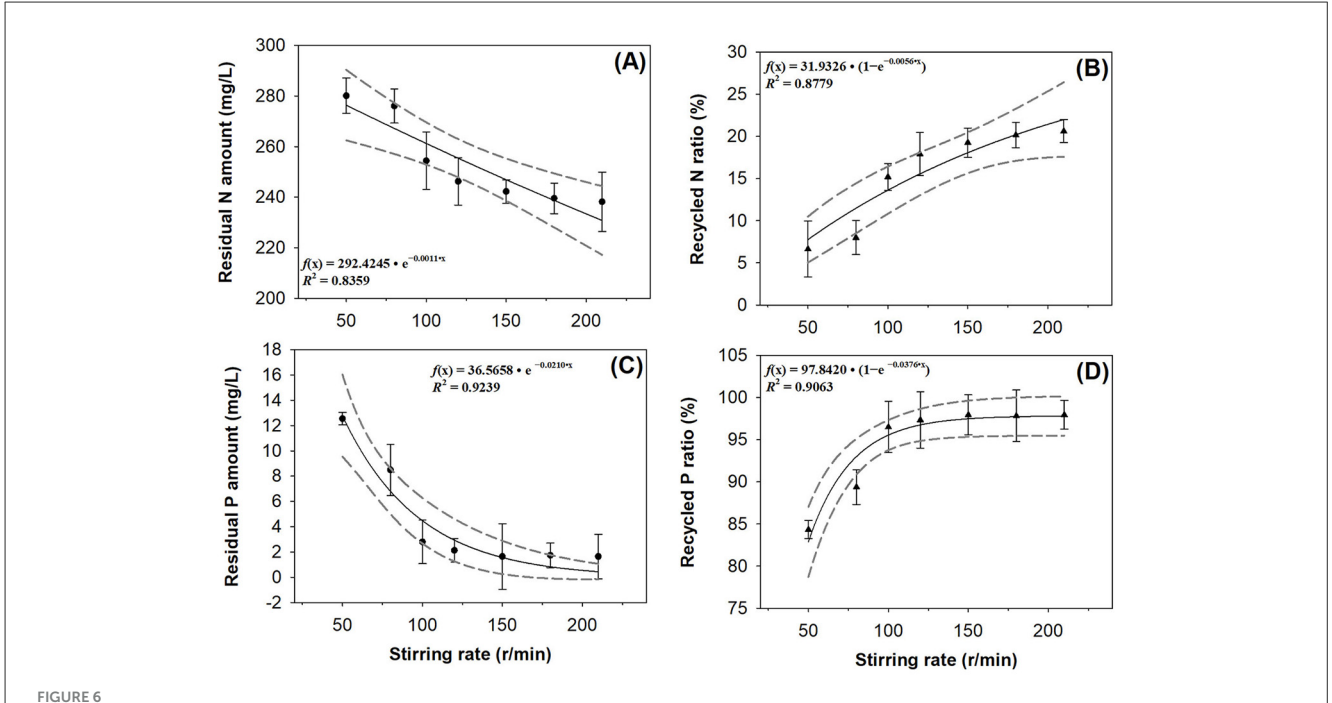
recovery rate at the same level for each factor, the optimal recovery process combination for struvite crystallization was a pH value of 10.50, aquatic temperature of  $30^{\circ}$ C, reaction time of 35 min (consistent with single-factor experimental results), stirring rate of  $180 \text{ r min}^{-1}$ , and Mg/P molar ratio of 2.0.

The  $R^2$  values increased in the following order: Mg/P molar ratio > pH > aquatic temperature > reaction time > stirring rate). The order of significance for the factors affecting the  $PO_4^{3-}$ -P recovery rate was Mg/P molar ratio > pH value > aquatic temperature > reaction time > stirring rate. It can be concluded that the main factors influencing the  $PO_4^{3-}$ -P recovery rate were the Mg/P molar ratio and pH, whereas the secondary factors were aquatic temperature, reaction time, and stirring rate.

According to the average  $PO_4^{3-}$ -P recovery rate at the same level for each factor in the orthogonal experimental results, the optimal recovery process combinations for struvite crystallization were 9.50, aquatic temperature of 20°C, reaction time of 30 min, stirring rate of 150 r min<sup>-1</sup>, and 2.0, respectively.

## Analysis of surface characteristics of recovered struvite particles under the optimal process conditions

The optimal scheme obtained from the orthogonal experiment is verified using a validation test. The resulting crystalline precipitate was filtered using a filter paper, placed in an oven, and dried at 40°C for 48 h. The dried material was subjected to X-ray diffraction (XRD) analysis, and the results are shown in Figure 7. The XRD pattern of the struvite



Amounts and recycled ratios of nitrogen (N) and phosphorus (P) in post-experiment residuals (A, C) during the process where N and P were recycled (B, D) in response to stirring rates. Plots mark means with boxes being representative for N and triangles for P. Error bars represent standard errors. The full lines mark the fit curves, with dashed lines framing the 95% confidence bands.

precipitate was compared to the standard diffraction pattern of MgNH $_4$ PO $_4$ ·6H $_2$ O (PTF card 15-0762). The XRD pattern of the struvite crystals generated under optimal conditions closely matched the characteristic peaks of the standard struvite card, indicating that the main component of the precipitate was the struvite crystals (Figure 7). Additionally, the purity of the struvite recovered under optimal conditions was 99.35%.

The SEM images of the struvite particles are shown in Figure 8. At 500× magnification, the former struvite crystals appeared rod-shaped (Figure 8A). At 1,000× magnification, the surface of the recovered product showed the presence of adherent substances (Figure 8B). At a higher magnification of 5,000×, this phenomenon was more clearly observed and layered structures within the particles were visible (Figure 8C). Energy-dispersive spectroscopy (EDS) analysis revealed that the primary characteristic peaks of the recovered products were O, Mg, and P (Figure 8D). This further confirmed that the main component of the recovered precipitate was struvite crystals.

The results of the EDX elemental quantitative analysis are listed in Table 3. The atomic percentage of Ca was only 0.12, indicating that Ca impurities precipitated. It was formed from  $\text{Ca}^{2+}$  in tap water that reacted with  $\text{PO}_4^{3-}$ , and both resulted in a trace amount of  $\text{Ca3}(\text{PO4})_2 \cdot \text{xH}_2\text{O}$ , which is consistent with the previously determined purity results. The molar ratio of Mg/P was 1.15, suggesting the presence of other trace Mg salt impurities such as Mg(OH)<sub>2</sub> precipitates, in addition to struvite.

#### Discussion

# N removal from wastewater in response to single-factor experiments

The single-factor experiments conducted in this study elucidated the nuanced responses of N removal from cornstarch wastewater via struvite crystallization. The experimental process highlighted the influence of a single factor: pH, Mg/P molar ratio, aquatic temperature, reaction time, and stirring rate. Specifically, residual N exhibited a symmetric power curve response to pH, approaching a minimum near pH 11.10. These findings align with those of previous studies, which suggested that pH significantly governed struvite solubility and precipitation efficiency, with optimal N removal typically occurring around pH 9.5-10.5 due to enhanced ammonia availability for struvite formation (Zeng et al., 2021; Zhao et al., 2024). This pH range was close to the minimum amount of N removal, and the difference between the studies resulted from variations in the reaction performance of the wastewater types. However, the unusually high inflection point observed in this study may reflect specific wastewater characteristics such as high ammonium concentrations, necessitating further investigation.

The Mg/P molar ratio influenced the amount of residual N through an exponential decay curve with a decay rate of 0.0214. The recycled N ratio followed an exponentially increasing trend, reaching a theoretical maximum of 29.23%. These corroborate studies demonstrating that an Mg/P ratio above 1:1 ensures sufficient magnesium for struvite crystal formation, thereby

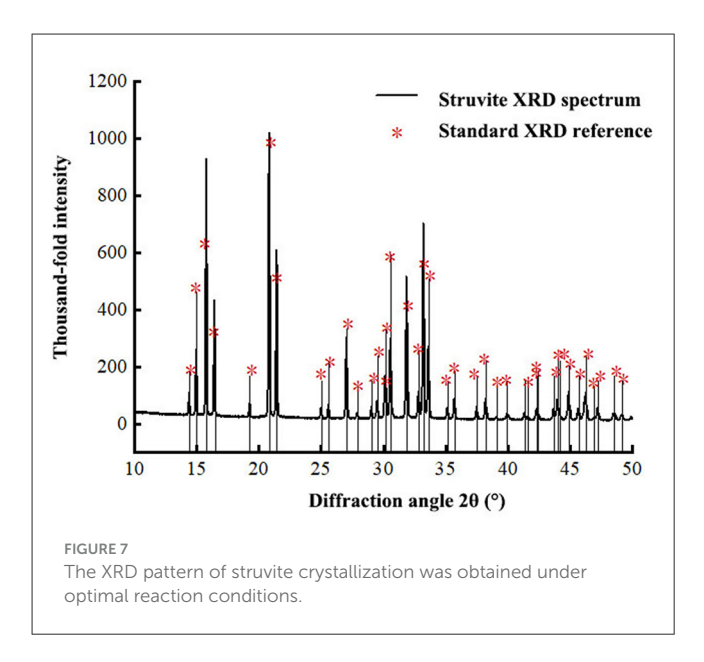
TABLE 2 Results of the orthogonal experiment.

Experiment number	А	В	С	D	E	$NH_4^+ ext{-}N$ Recovery	$PO^{3-}_4 ext{-P}$ Recovery
	рН	Mg <sup>/</sup> P molar ratio	Aquatic temperature (°C)	Stirring rate $(r \cdot min^{-1})$	Reaction time (min)	%	%
1	9.00	1.4	15	100	20	9.34	87.70
2	9.00	1.6	20	120	30	14.75	94.09
3	9.00	1.8	25	150	35	19.27	96.99
4	9.00	2.0	30	180	40	23.32	96.38
5	9.50	1.4	20	150	40	19.72	96.86
6	9.50	1.6	15	180	35	20.62	96.99
7	9.50	1.8	30	100	30	23.78	95.54
8	9.50	2.0	25	120	20	19.72	95.78
9	10.00	1.4	25	180	30	23.78	95.42
10	10.00	1.6	30	150	20	18.81	92.28
11	10.00	1.8	15	120	40	19.72	98.55
12	10.00	2.0	20	100	35	22.87	98.07
13	10.50	1.4	30	120	35	27.83	83.24
14	10.50	1.6	25	100	40	26.48	89.87
15	10.50	1.8	20	180	20	22.87	93.85
16	10.50	2.0	15	150	30	22.87	97.83
K11	16.67	20.17	18.14	20.62	17.69		
K12	20.96	20.17	20.05	20.51	21.29		
K13	21.29	21.41	22.31	20.17	22.65		
K14	25.02	22.20	23.44	22.65	22.31		
K21	93.79	90.81	95.27	92.79	92.40		
K22	96.29	93.31	95.72	92.92	95.72		
K23	96.08	96.23	94.51	95.99	93.82		
K24	91.20	97.02	91.86	95.66	95.42		
R1	8.35	2.03	5.30	2.48	4.96		
R2	5.09	6.21	3.86	3.20	3.32		

enhancing N recovery (Zheng et al., 2018; Zin and Kim, 2021). For example, the study of Zin and Kim (2021) demonstrated that using a Mg/P molar ratio of about 1:1 in the presence of Mg-biochar significantly enhanced struvite formation, which recovered 92.2% of PO<sub>4</sub><sup>3</sup>-P and 54.8% of NH<sub>4</sub><sup>+</sup>-N from food wastewater and sewage sludge ash (Zin and Kim, 2021). In our study, aquatic temperature affected residual N via a symmetric power curve that predicted zero residual N at 49.07°C. The recycled N ratio followed a sigmoid function with a midpoint at 191.05°C, which far exceeded practical temperatures. This suggests limited practical impacts of the solution temperature within the tested range (5–40°C), which is consistent with the findings that optimal struvite formation occurs at 25–30°C (Zhang et al., 2020).

The reaction time exhibited an exponential decay in residual N at a rate of 0.0048 and an exponential increase in the recycled N ratio (up to a maximum of 29.41%). These results are consistent

with those of previous studies, which indicated that a longer reaction time can enhance N removal by promoting sufficient crystal growth (Yang et al., 2024). Similarly, the stirring rate exponentially reduced the residual N (rate 0.0011) and increased the recycled N ratio to 31.93%, which supports the evidence that adequate stirring can promote homogeneous mixing and crystal formation (Zhai et al., 2022). The fitted curves for Mg/P, reaction time, and stirring rate can be described by exponential models, and the fitted curves for pH and temperature can be described by sigmoidal or power models. Together, these factors contribute to the reflection of the complex interactions between chemical kinetics and physical conditions. These findings are consistent with those of previous studies on the struvite precipitation dynamics (Zhou et al., 2024; Zhu et al., 2020). These results underscore the need for the precise control of these facets through sensorbased monitoring systems to optimize N recovery and minimize



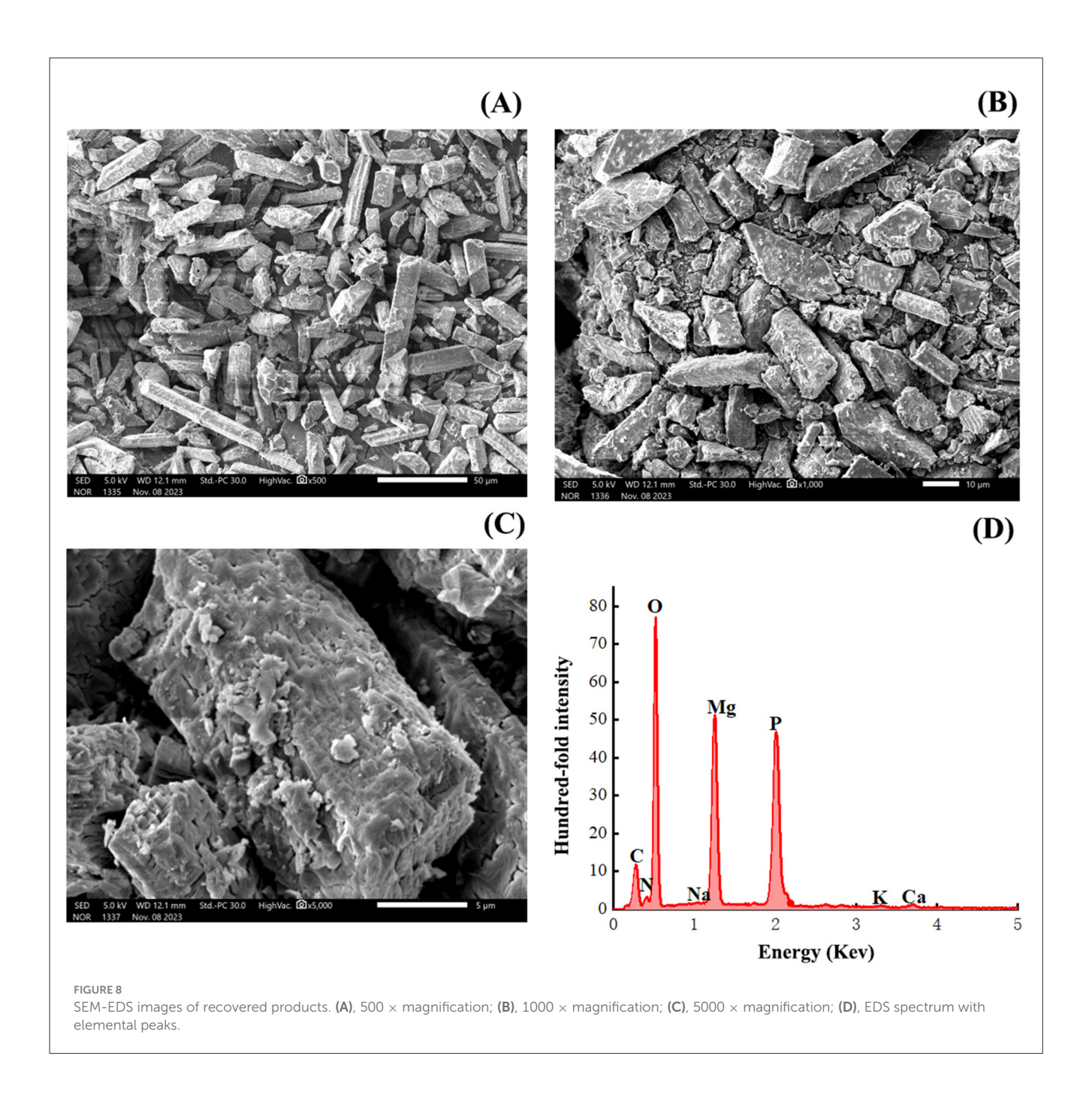
environmental impacts. This was highlighted by the high purity (99.35%) of the struvite obtained under the optimal conditions in this study.

# P removal from wastewater in response to single-factor experiments

The findings of this study confirm that struvite crystallization is a viable approach for recovering P from cornstarch wastewater, which aligns with the principles of circular economy by transforming waste into a valuable resource (Achilleos et al., 2022). The recovery rates of PO<sub>4</sub><sup>3-</sup>-P can be as high as 98.52%, which is higher than that of NH<sub>4</sub><sup>+</sup>-N (up to 31.93%) under optimized conditions, underscoring the potential of struvite as a slow-release fertilizer. This P recovery rate was comparable to that reported by Wang et al. (2021); however, the N recovery rate in the present study was much lower. The use of a sensor-equipped facility enabled precise control of reaction conditions that further enhanced the process efficiency and product purity by removing P. This was verified by XRD and SEM-EDS analyses, which corroborated previous studies demonstrating the efficacy of struvite for nutrient recovery from various waste streams, such as swine manure (Zhang et al., 2020) and urine (Zheng et al., 2018). The orthogonal experiment revealed that pH and the Mg/P molar ratio were the most significant factors influencing P recovery, whereas pH and aquatic temperature were more critical for N recovery. These conditions are consistent with findings that emphasize the importance of these parameters in struvite formation (Zeng et al., 2021; Zhao et al., 2024). For example, a pot experiment validated the agronomic potential of recovered struvite, with results unraveled through enhanced plant growth compared to superphosphate, which can be explained by the slow-release properties (Li et al., 2025). However, challenges existed in results caused by factors such as the trace impurities of calcium phosphate [Ca3(PO4)<sub>2</sub>]. Precise sensor-based monitoring is required in future research to optimize scalability and cost-effectiveness (Zhu et al., 2020; Zin and Kim, 2021).

The single-factor experiments provided detailed insights into the P removal dynamics in response to the pH, Mg/P molar ratio, water temperature, reaction time, and stirring rate. The exponential decay curve for the amount of residual P with increasing pH reached a minimum at pH 11.05, which reflects the enhanced solubility and precipitation of struvite at higher pH levels (Zhou et al., 2024). The rise-to-maximum exponential function for 100% recycled P ratio peaked at pH 11.05, which aligns with results indicating optimal struvite formation around pH 9.5-10.5 (Zeng et al., 2021). The exponential decay of residual P and the riseto-maximum curve for recycled P (98.52% at an Mg/P molar ratio of 3.00) indicated that adequate Mg availability is essential for effective P precipitation. According to a study by Zhu et al. (2020), MgO-biochar (synthesized via fast pyrolysis of MgCl<sub>2</sub>impregnated corn stalks) achieved a 99% phosphate removal rate from a 198.705 mg P/L solution, which endorsed the critical role of magnesium availability in effective phosphorus precipitation with evidence by the formation of Mg3(PO4)2 and MgHPO4 precipitates at an optimal Mg/P molar ratio (Zhu et al., 2020). The quadratic polynomial curve for P removal with respect to aquatic temperature and temperature peaked at 25.72°C that resulting in a 98.12% recovery rate. This indicates an optimal temperature range for reaction kinetics, which is consistent with the findings of Zhao et al. (2024). The exponential decay of residual P increased with the reaction time and was coupled with a maximum recycled P ratio of 96.95% in 60 min. This highlights the importance of adequate reaction duration, as noted by Zin and Kim (2021). Similarly, the exponential decay of residual P went with the increase in stirring rate and reached a 97.84% recovery at 210 r·min<sup>1</sup>. This underscores the role of homogeneous mixing in crystal growth and explains the findings of Yang et al. (2024). These curve characteristics together contributed to the higher recovery rates for both N and P, which were attributed to the integrated sensor system and real-time optimization of multifaceted reaction conditions (Zhai et al., 2022; Zhang S. J. et al., 2023). Future studies should explore the scalability of sensor-based systems and long-term stability of struvite under diverse soil conditions to further enhance its practical application.

In the single factor of pH mediation, error bars for recycled P presented standard errors, which resulted in large variations in treatments with pH values of 8.5, 9.0, and 9.5, caused by large variations among replicated observations. This variability likely stems from the sensitivity of struvite crystallization to pH, which significantly influences the solubility and precipitation efficiency of P in struvite (MgNH4PO4·6H2O). At pH 8.5-9.5, struvite formation was highly sensitive to pH fluctuations, even within a small range. This pH range is close to the optimal pH range (approximately 9.0-10.0) for precipitation, where slight deviations can cause inconsistent crystal formation or dissolution. These inconsistent pH values can be critical because they straddled the threshold where struvite solubility shifted and led to variable P recycling rates. Factors such as inconsistent mixing, sensor calibration errors, and minor variations in wastewater composition (e.g., ion concentrations) could amplify this variability and result in large standard errors. The study noted that pH is a primary factor



affecting recovery rates, and orthogonal experiments confirmed its significant impact. At these pH levels, the sensitivity of the system to external conditions likely caused the high variability observed. Overall, the high variation in the recycled P ratio is reasonable; however, future work is suggested to overcome this variability.

# N and P removals from wastewater in response to multi-factor experiments

This study elucidated the efficacy of struvite crystallization for N and P recovery from cornstarch wastewater, which aligns with the need for sustainable nutrient management in agroindustrial

systems. The experimental design incorporated both single-factor and orthogonal experiments, which together provided a robust framework for identifying key factors influencing struvite precipitation. The use of sensors for real-time monitoring of pH,  ${\rm Mg^{2+}}$ , and  ${\rm PO_4^{3-}}$  concentrations ensured optimal reaction conditions and minimized chemical inputs and sludge production. This approach contrasts with conventional chemical precipitation methods, which often generate secondary contaminants (Mohan et al., 2020). The high purity of the recovered struvite (99.35%) was confirmed by XRD and SEM-EDS analyses, which highlights its suitability as a slow-release fertilizer and offers a sustainable alternative to conventional phosphate fertilizers (Zhou et al., 2024).

The optimal conditions for NH<sub>4</sub><sup>+</sup>-N recovery were determined to be a combination of factors at a pH of 10.50, Mg/P molar

TABLE 3 EDX element quantitativean alysis results.

Element	Atomic percent (%)		
С	$32.21 \pm 0.2$		
N	$2.94 \pm 0.14$		
О	$44.97 \pm 0.24$		
Na	$0.15\pm0.02$		
Mg	$10.23 \pm 0.07$		
P	$9.12 \pm 0.06$		
K	$0.26\pm0.01$		
Ca	$0.12\pm0.01$		
Total	100		

ratio of 2.0, aquatic temperature of 30°C, reaction time of 35 min, and stirring rate of 180 rpm. Otherwise, the optimization for PO<sub>4</sub><sup>3</sup>-P was characterized by a combination of pH of 9.50, Mg/P molar ratio of 2.0, aquatic temperature of 20°C, reaction time of 30 min, and stirring rate of 150 r·min<sup>1</sup>. These conditions yielded NH<sub>4</sub><sup>+</sup>-N and PO<sub>4</sub><sup>3</sup>-P recovery rates of up to 27.83% and 98.55%, respectively, surpassing those reported in similar studies using biochar or algal systems (Mohsenpour et al., 2021; Zhu et al., 2020). Compared to the results of 99.2% P recovery from swine manure via catalytic-thermal hydrolysis found by Zhang et al. (2020), our study demonstrated a comparable P recovery with lower energy inputs due to sensor-driven optimization. However, our N recovery remains lower than that in previous systems, such as the case reported by Yang et al. (2024), where N recovery of 89% was obtained through bipolar membrane electrodialysis.

The struvite crystals exhibited a rod-shaped morphology and high purity, which is consistent with the findings of Zheng et al. (2018), who noted enhanced N and P recovery with biocharassisted struvite precipitation. The rod-shaped morphology of the struvite crystals likely resulted from a controlled crystallization process influenced by the specific concentrations and ratios of magnesium, ammonium, and phosphate ions in corn-processing wastewater. This controlled environment was coupled with efficient precipitation conditions that favored the formation of struvite. Pot experiments confirmed the fertilizer potential of the recovered struvite, which concurs with the results of efficacy in vegetable growth (Li et al., 2025). These results advocate scaling up sensorintegrated struvite crystallization systems to address nutrient pollution, while promoting resource recovery. They also offer a model for sustainable wastewater management in the corn processing industry.

# The surface feature characteristics of post-experiment struvite

The surface characteristics of the struvite crystals recovered from cornstarch wastewater were analyzed using XRD, SEM, and EDS. Surface features provide critical insights into their composition and potential as fertilizers. The XRD patterns confirmed that the precipitate consisted primarily of struvite with

a purity of 99.35%, which closely aligned with the standard diffraction pattern (PTF card 15-0762). This high purity is consistent with findings from studies on struvite precipitation from nutrient-rich wastewater, where controlled pH and molar ratios enhance crystal formation (Zhang et al., 2020; Zheng et al., 2018). SEM images revealed rod-shaped crystals at 500× magnification, with layered structures and adhered substances visible at higher magnifications (1,000× and 5,000×, respectively). These morphological features corroborate the observations of struvite used for nutrient recovery from swine manure, where struvite exhibited similar rod-like structures under optimized conditions (Zhang et al., 2020). EDS analysis identified the dominant elements (O, Mg, and P) and trace impurities, such as Ca (0.12%). This suggests minor calcium phosphate formation, which is a common byproduct of wastewater containing tap water (Zeng et al., 2021). A Mg/P molar ratio of 1.15 indicates potential Mg(OH)<sub>2</sub> impurities, which is in agreement with previous studies on urine-derived struvite (Zhang B. et al., 2023). Compared to biochar-based struvite recovery ( $\sim$ 88.0%), which often shows lower purity due to high adsorption variability (Zhou et al., 2024; Zhu et al., 2020), our sensor-controlled precipitation achieved superior crystal quality. These characteristics enhance the applicability of struvite as a slow-release fertilizer, as validated by pot experiments showing improved plant growth (Zhao et al., 2024). The integration of real-time sensor monitoring is likely to minimize impurities and advance nutrient recovery systems.

The recovered struvite exhibited rod-shaped morphology, which was confirmed by SEM with EDS at 5-20 kV. It was revealed with high purity (98.55%) and a specific spectrum of elemental composition (Mg, P, and N). To further elucidate the microscopic morphology, Transmission Electron Microscopy (TEM, JEOL JEM-2100F, 200 kV) was employed to visualize the nanoscale crystal structure of struvite to reveal the lattice fringes and confirm the rod-shaped morphology. Brunauer-Emmett-Teller (BET) analysis (Micromeritics ASAP 2020) can be used to measure the surface area and pore size distribution of struvite, depending on its suitability for slow-release fertilizer applications. These approaches were suggested by Zheng et al. (2018), who highlighted that the controlled crystallization process is influenced by specific concentrations of magnesium, ammonium, and phosphate ions in corn-processing wastewater, enhancing the potential of struvite for sustainable nutrient recovery.

# Applicative suggestions for using struvite in N and P removals in corn wastewater

The present study demonstrated the efficacy of struvite crystallization for N and P recovery from cornstarch wastewater, achieving high recovery rates and producing a high-purity struvite product suitable as a slow-release fertilizer. These results support previous findings that struvite precipitation can effectively mitigate the risk of eutrophication by reducing the nutrient discharge (Zeng et al., 2021). The orthogonal experimental design revealed that pH and Mg/P molar ratio are critical for optimizing PO<sub>4</sub><sup>3-</sup>-P recovery, while pH and aquatic temperature significantly influence NH<sub>4</sub><sup>4</sup>-N recovery. These findings corroborate earlier research emphasizing

the precise control of reaction conditions to maximize struvite yield (Wang et al., 2023; Zhao et al., 2024).

The high purity (99.35%) of the recovered struvite was confirmed by XRD and SEM-EDS analyses, which underscores its potential for agricultural reuse, consistent with studies highlighting struvite slow-release properties (Li et al., 2025). The rod-shaped crystal morphology observed enhanced its applicability as a fertilizer, but the trace impurities [like Ca3(PO4)<sub>2</sub>] suggest a need for further refinement to eliminate secondary precipitates, as noted in nutrient recovery studies (Zhang B. et al., 2023). Compared to conventional chemical precipitation, struvite crystallization reduces sludge production and chemical inputs, offering a sustainable alternative strategy compared to conventional methodology (Zhai et al., 2022). The integration of biochar or algal systems was explored in prior studies, and their results were further enhanced in our study for nutrient capture, but they faced challenges such as adsorption variability or high harvesting costs, as mentioned by previous scholars (Mohsenpour et al., 2021; Zhu et al., 2020). The abiotic approach used in this study avoided such biotic limitations and ensured more stable performance.

A sensor-based system was used to monitor the pH, Mg/P ratio, aquatic temperature, reaction time, and stirring rate, which together enabled real-time optimization to synthesize the best conditions for these facets. Their combination can improve efficiency and reduce energy costs, which is essential for industrial popularization because high precision can meet advancements in sensor-driven wastewater treatment (Zheng et al., 2023). The adaptability of the system to influent variability supports its scalability for industrial applications.

Policies should incentivize struvite recovery facilities and integrate sensor technologies for process control to promote N and P recycling in the corn deep-processing industry. Subsidies can be considered for adopting waste-derived fertilizers and regulations enforcing nutrient discharge limits that may have driven the adoption of circular economic principles (Bermúdez et al., 2024). Future research should focus on cost-effective sensor integration and long-term field trials to validate the agricultural benefits of struvite.

#### Conclusion

This study explored struvite crystallization as a sustainable method to recover N and P from cornstarch wastewater, with the aim of addressing eutrophication risks and promoting circular economic principles. This study utilized a sensor-equipped facility to optimize the reaction conditions and achieve high-purity struvite for potential use as a slow-release fertilizer. This study employed both single-factor and orthogonal experiments to identify the optimal conditions for N and P recovery. Key factors that influence the recovery rate include pH, Mg/P molar ratio, aquatic temperature, reaction time, and stirring rate. For NH<sub>4</sub><sup>+</sup>-N, the optimal recovery (up to 27.83%) occurred under the combined conditions of pH 10.50, Mg/P ratio of 2.0, 30°C, reaction time of 35 min, and stirring at 180 rpm. For PO<sub>4</sub><sup>3</sup>-P, however, the optimal recovery was much higher up to 98.55% which was achieved at another combination of facets in pH 9.50, Mg/P

ratio of 2.0, aquatic temperature at 20°C, reaction in 30 min, and stirring at 150 r·min<sup>1</sup>. Both were attributed to the employment of a sensor-based monitoring system that ensured precise control, minimized chemical inputs, and controlled sludge production compared to conventional methods. XRD, SEM, and EDS analyses confirmed the high purity of the recovered struvite (99.35%) and its rod-shaped morphology with minimal impurities, such as calcium phosphate. These characteristics together enhance their suitability as controlled-release fertilizers in theory, supported by prior botanical studies. This approach outperformed biochar and algal systems by avoiding adsorption variability and high harvesting costs. Overall, these findings advocate scaling up sensorintegrated struvite crystallization in corn-processing industries to mitigate nutrient pollution and recover resources. Policy incentives, cost-effective sensor integration, and long-term field trials are recommended for promoting sustainable wastewater management and agricultural reuse.

## Data availability statement

The original contributions presented in the study are included in the article/supplementary material, further inquiries can be directed to the corresponding author.

#### **Author contributions**

HL: Conceptualization, Funding acquisition, Methodology, Writing – review & editing. YH: Data curation, Formal analysis, Methodology, Software, Writing – original draft. BL: Conceptualization, Funding acquisition, Writing – review & editing. XL: Funding acquisition, Supervision, Writing – review & editing. XT: Formal analysis, Writing – review & editing. SL: Validation, Writing – review & editing. LM: Validation, Writing – review & editing.

# **Funding**

The author(s) declare that financial support was received for the research and/or publication of this article. This research was funded by Jilin Provincial Department of Science and Technology with the Grant Number 20220203005SF in the program namely Science and Technology Development Plan Project of Jilin Province.

# Acknowledgments

Authors acknowledge editors and peer reviewers who make essential contributions to the current edition of this manuscript.

#### Conflict of interest

YH was employed by China Construction Xinjiang Construction Engineering Group Third Construction Engineering Co., Ltd., Urumqi, China. XL was employed by China Northeast Municipal Engineering Design and Research Institute Co., Ltd.

The remaining authors declare that the research was conducted in the absence of any commercial or financial relationships that could be construed as a potential conflict of interest.

#### Generative Al statement

The author(s) declare that no Gen AI was used in the creation of this manuscript.

Any alternative text (alt text) provided alongside figures in this article has been generated by Frontiers with the support of artificial intelligence and reasonable efforts have been made to ensure accuracy, including review by the authors wherever possible. If you identify any issues, please contact us.

#### Publisher's note

All claims expressed in this article are solely those of the authors and do not necessarily represent those of their affiliated organizations, or those of the publisher, the editors and the reviewers. Any product that may be evaluated in this article, or claim that may be made by its manufacturer, is not guaranteed or endorsed by the publisher.

## References

Aamir, M., and Hassan, M. (2025). Influences of granular activated carbon on methane production performance of cow manure and corn straw in semi-continuous stirring tank reactor: organic loading rate optimization and economic considerations. *Waste Biomass Valorization* 16, 4173–4185. doi: 10.1007/s12649-025-02983-0

Achilleos, P., Roberts, K. R., and Williams, I. D. (2022). Struvite precipitation within wastewater treatment: a problem or a circular economy opportunity? *Heliyon* 8:e09862. doi: 10.1016/j.heliyon.2022.e09862

Adetunji, C. O., Hefft, D. I., Jeevanandam, J., and Danquah, M. (2023). Next Generation Nanochitosan: Applications in Animal Husbandry, Aquaculture and Food Conservation. Cambridge, MA: Academic Press, Elsevier Inc.

Aguado, D., Montoya, T., Ferrer, J., and Seco, A. (2006). Relating ions concentration variations to conductivity variations in a sequencing batch reactor operated for enhanced biological phosphorus removal. *Environ. Model. Softw.* 21, 845–851. doi: 10.1016/j.envsoft.2005.03.004

Aguilar-Pozo, V. B., Chimenos, J. M., Elduayen-Echave, B., Olaciregui-Arizmendi, K., López, A., Gómez, J., et al. (2023). Struvite precipitation in wastewater treatment plants anaerobic digestion supernatants using a magnesium oxide by-product. *Sci. Total Environ.* 890:164084. doi: 10.1016/j.scitotenv.2023.164084

Aka, R. J. N., Hossain, M. M., Nasir, A., Zhan, Y. H., Zhang, X. Y., Zhu, J., et al. (2024). Enhanced nutrient recovery from anaerobically digested poultry wastewater through struvite precipitation by organic acid pre-treatment and seeding in a bubble column electrolytic reactor. *Water Res.* 252:121239. doi: 10.1016/j.watres.2024.121239

Alatawi, I. S. S., Almughathawi, R., Madkhali, M. M. M., Alshammari, N. M., Alaysuy, O., Mogharbel, A. T., et al. (2025). Sustainable waste-derived cellulose-based nanosensor for cobalt ion detection, removal, and recovery from industrial effluents and battery wastes. *J. Water Process Eng.* 70:106974. doi: 10.1016/j.jwpe.2025.106974

Bermúdez, L. A., Mendoza, V. D., Díaz, J. C. L., Pascual, J. M., del Mar Muñio Martínez, M., and Capilla, J. M. P. (2024). Investigation of the agricultural reuse potential of urban wastewater and other resources derived by using membrane bioreactor technology within the circular economy framework. Sci. Total Environ. 955:177011. doi: 10.1016/j.scitotenv.2024.177011

Casellas, M., Dagot, C., and Baudu, M. (2006). Set up and assessment of a control strategy in a SBR in order to enhance nitrogen and phosphorus removal. *Process Biochem.* 41, 1994–2001. doi: 10.1016/j.procbio.2006.04.012

CDC (2024). Harmful Algal Bloom (HAB)-Associated Illness. Available online at: https://www.cdc.gov/harmful-algal-blooms/causes/index.html (accessed March 4, 2025).

Chamas, A., Moon, H., Zheng, J., Qiu, Y., Tabassum, T., Jang, J. H., et al. (2020). Degradation rates of plastics in the environment. ACS Sustain. Chem. Eng. 8, 3494–3511. doi: 10.1021/acssuschemeng.9b06635

Dong, M., He, L., Jiang, M., Zhu, Y., Wang, J., Gustave, W., et al. (2023). Biochar for the removal of emerging pollutants from aquatic systems: a review. *Int. J. Environ. Res. Public Health* 20:1679. doi: 10.3390/ijerph20031679

Fendel, V., Maurer, C., Kranert, M., Huang, J. J., and Schäffner, B. (2022). The potential of the co-recycling of secondary biodegradable household resources including wild plants to close nutrient and carbon cycles in agriculture in Germany. *Sustainability* 14:5277. doi: 10.3390/su14095277

Geng, M. X., Zeng, T., Deng, X. Y., Zhang, Z. Y., Xiao, C. Q., and Chi, R. A. (2024). Innovative strategies for ammonia nitrogen removal in rare earth tailings: an advanced element recycling process using leaching, chemical

precipitation and adsorption. J. Water Process Eng. 67:106205. doi: 10.1016/j.jwpe.2024. 106205

He, L. T., Wang, D. H., Wu, Z. Y., Lv, Y. Z., and Li, S. C. (2022). Magnesium-modified biochar was used to adsorb phosphorus from wastewater and used as a phosphorus source to be recycled to reduce the ammonia nitrogen of piggery digestive wastewater. *J. Clean. Prod.* 360:132130. doi: 10.1016/j.jclepro.2022.132130

How, S. W., Chua, A. S. M., Ngoh, G. C., Nittami, T., and Curtis, T. P. (2019). Enhanced nitrogen removal in an anoxic-oxic-anoxic process treating low COD/N tropical wastewater: low-dissolved oxygen nitrification and utilization of slowly-biodegradable COD for denitrification. *Sci. Total Environ.* 693:133526. doi: 10.1016/j.scitotenv.2019.07.332

Jaramillo, F., Orchard, M., Muñoz, C., Zamorano, M., and Antileo, C. (2018). Advanced strategies to improve nitrification process in sequencing batch reactors - a review. *J. Environ. Manage.* 218, 154–164. doi: 10.1016/j.jenvman.2018. 04.019

Kim, B. H., Choi, J. E., Cho, K., Kang, Z., Ramanan, R., Moon, D. G., et al. (2018). Influence of water depth on microalgal production, biomass harvest, and energy consumption in high rate algal pond using municipal wastewater. *J. Microbiol. Biotechnol.* 28, 630–637. doi: 10.4014/jmb.1801.01014

Kim, K.-S., Yoo, J.-S., Kim, S., Lee, H. J., Ahn, K.-H., and Kim, I. S. (2007). Relationship between the electric conductivity and phosphorus concentration variations in an enhanced biological nutrient removal process. *Water Sci. Technol.* 55, 203–208. doi: 10.2166/wst.2007.053

Kowalczuk, D., and Pitucha, M. (2019). Application of FTIR method for the assessment of immobilization of active substances in the matrix of biomedical materials. *Materials* 12:2972. doi: 10.3390/ma12182972

Lessmann, M., Kanellopoulos, A., Kros, J., Orsi, F., and Bakker, M. (2023). Maximizing agricultural reuse of recycled nutrients: a spatially explicit assessment of environmental consequences and costs. *J. Environ. Manage.* 332:117378. doi: 10.1016/j.jenvman.2023.117378

Li, B., Huang, H. M., Boiarkina, I., Yu, W., Huang, Y. F., Wang, G. Q., et al. (2019). Phosphorus recovery through struvite crystallisation: recent developments in the understanding of operational factors. *J. Environ. Manage.* 248:109254. doi: 10.1016/j.jenvman.2019.07.025

Li, Y., Wang, W., Cui, J., Liu, X., and Liu, J. (2025). A full chain of applying struvite recovered from biogas slurry to promote vegetable growth. *Agriculture* 15:1352. doi: 10.3390/agriculture15131352

Liu, Y., Kwag, J.-H., Kim, J.-H., and Ra, C. (2011). Recovery of nitrogen and phosphorus by struvite crystallization from swine wastewater. *Desalination* 277, 364–369. doi: 10.1016/j.desal.2011.04.056

Luzzi, S. C., Gardner, R. G., and Heins, B. J. (2024). The use of *Chlorella species* to remove nutrients from dairy wastewater to produce livestock feed. *Sustainability* 16:1382. doi: 10.3390/su16041382

Mohan, T., Shaheen, S. F. N., Swathi, K. V., Sowmya, A., and Ramani, K. (2020). Sustainable biological system for the removal of high strength ammoniacal nitrogen and organic pollutants in poultry waste processing industrial effluent. *J. Air Waste Manag. Assoc.* 70, 1236–1243. doi: 10.1080/10962247.2020.1731013

Mohsenpour, S. F., Hennige, S., Willoughby, N., Adeloye, A., and Gutierrez, T. (2021). Integrating micro-algae into wastewater treatment: a review. *Sci. Total Environ.* 752:142168. doi: 10.1016/j.scitotenv.2020.142168

- Mugwili, M. E., Waanders, F. B., Masindi, V., and Fosso-Kankeu, E. (2023). Effective removal of ammonia from aqueous solution through struvite synthesis and breakpoint chlorination: insights into the synergistic effects of the hybrid system. *J. Environ. Manage.* 334:117506. doi: 10.1016/j.jenvman.2023.117506
- Nobaharan, K., Bagheri Novair, S., Asgari Lajayer, B., and van Hullebusch, E. D. (2021). Phosphorus removal from wastewater: the potential use of biochar and the key controlling factors. *Water* 13:517. doi: 10.3390/w13040517
- Noriega-Hevia, G., Serralta, J., Seco, A., and Ferrer, J. (2023). A pH-based control system for nitrogen recovery using hollow fibre membrane contactors. *J. Environ. Chem. Eng.* 11:110519. doi: 10.1016/j.jece.2023.110519
- Oliveira, V., Dias-Ferreira, C., González-García, I., Labrincha, J., Horta, C., and García-González, M. C. (2021). A novel approach for nutrients recovery from municipal waste as biofertilizers by combining electrodialytic and gas permeable membrane technologies. *Waste Manag.* 125, 293–302. doi: 10.1016/j.wasman.2021.02.055
- Patel, V., Akbar, M. A., Kruse, P., and Selvaganapathy, P. R. (2023). A reagent-free phosphate chemiresistive sensor using carbon nanotubes functionalized with crystal violet. *Analyst* 148, 3551–3558. doi: 10.1039/d3an00622k
- Pesonen, J., Sauvola, E., Hu, T., and Tuomikoski, S. (2020). Use of side stream-based MgSO4 as chemical precipitant in the simultaneous removal of nitrogen and phosphorus from wastewaters. *Desalin. Water Treat.* 194, 389–395. doi: 10.5004/dwt.2020.26037
- Petrea, S. M., Simionov, I. A., Antache, A., Nica, A., Oprica, L., Miron, A., et al. (2023). An analytical framework on utilizing various integrated multi-trophic scenarios for basil production. *Plants* 12:540. doi: 10.3390/plants12030540
- Qi, H. J., Li, B., Nie, J., Luo, Y. Z., Yuan, Y., and Zhou, X. X. (2024). Assessing the capabilities of UV-NIR spectroscopy for predicting macronutrients in hydroponic solutions with single-task and multi-task learning. *Agronomy* 14:1974. doi: 10.3390/agronomy14091974
- Rekaby, S. A., Awad, M., Majrashi, A., Ali, E. F., and Eissa, M. A. (2021). Corn cobderived biochar improves the growth of saline-irrigated quinoa in different orders of Egyptian soils. *Horticulturae* 7:221. doi: 10.3390/horticulturae7080221
- Rickard, J. (2023). Newly Identified Algal Strains Rich in Phosphorous Could Improve Wastewater Treatment. Available online at: https://www.nrel.gov/news/program/2023/newly-identified-algal-strains-rich-in-phosphorous-could-improve-wastewater-treatment.html (accessed March 4, 2025).
- Romero, V., Sant'Anna, C., Lavilla, I., and Bendicho, C. (2023). Fluorescent paper-based sensor integrated with headspace thin-film microextraction for the detection of acyclic N-nitrosamines following in situ photocatalytic decomposition. *Anal. Chim. Acta* 1239:340729. doi: 10.1016/j.aca.2022.340729
- Saidou, H., Korchef, A., Ben Moussa, S., and Ben Amor, M. (2009). Struvite precipitation by the dissolved CO2 degasification technique: impact of the airflow rate and pH. *Chemosphere* 74, 338–343. doi: 10.1016/j.chemosphere.2008.09.081
- Sajjad, M., Huang, Q., Khan, S., Nawab, J., Khan, M. A., Ali, A., et al. (2024). Methods for the removal and recovery of nitrogen and phosphorus nutrients from animal waste: a critical review. *Ecol. Front.* 44, 2–14. doi: 10.1016/j.chnaes.2023.05.003
- Santos, A. F., Mendes, L. S., Alvarenga, P., Gando-Ferreira, L. M., and Quina, M. J. (2024). Nutrient recovery via struvite precipitation from wastewater treatment plants: influence of operating parameters, coexisting ions, and seeding. *Water* 16:1675. doi: 10.3390/w16121675
- Shourjeh, M. S., Kowal, P., Drewnowski, J., Szelag, B., Szaja, A., and Łagód, G. (2020). Mutual interaction between temperature and DO set point on AOB and NOB activity during shortcut nitrification in a sequencing batch reactor in terms of energy consumption optimization. *Energies* 13:5808. doi: 10.3390/en13215808
- Sidorczuk, D., Kozanecki, M., Civalleri, B., Pernal, K., and Prywer, J. (2020). Structural and optical properties of struvite. Elucidating structure of infrared spectrum in high frequency range. *J. Phys. Chem. A* 124, 8668–8678. doi: 10.1021/acs.jpca.0c04707
- Siontorou, C. G., Georgopoulos, K. N., and Nalantzi, M. M. E. (2017). Designing biosensor networks for the environmental risk assessment of aquatic systems. *Crit. Rev. Environ. Sci. Technol.* 47, 40–63. doi: 10.1080/10643389.2016.12 78141
- Sniatała, B., Al-Hazmi, H. E., Sobotka, D., Zhai, J., and Makinia, J. (2024). Advancing sustainable wastewater management: a comprehensive review of nutrient recovery products and their applications. Sci. Total Environ. 937:173446. doi: 10.1016/j.scitotenv.2024.173446
- Strawn, D. G., Crump, A. R., Peak, D., Garcia-Perez, M., and Möller, G. (2023). Reactivity of Fe-amended biochar for phosphorus removal and recycling from wastewater. *PLOS Water* 2:e0000092. doi: 10.1371/journal.pwat.0000092
- Tarigan, N. B., Amal, M. Jr., Ekasari, J., Keesman, K. J., and Verdegem, M. (2025). Nitrogen, phosphorus, and carbon dynamics in biofloc system of Nile tilapia fed with high non-starch polysaccharides diet. *Aquaculture* 596:741714. doi:10.1016/j.aquaculture.2024.741714
- The Nature Conservacy (2025). Impacts of the Dead Zone: Algae Blooms in the Gulf Threaten Seafood Production, Recreation and Marine Life. Available online at: https://www.nature.org/en-us/about-us/where-we-work/priority-landscapes/gulf/stories-in-the-gulf/gulf-dead-zone/ (accessed March 4, 2025).

- Vunnava, V. S. G., and Singh, S. (2021). Integrated mechanistic engineering models and macroeconomic input-output approach to model physical economy for evaluating the impact of transition to a circular economy. *Energy Environ. Sci.* 14, 5017–5034. doi: 10.1039/d1ee00544h
- Wan, L. L., Cao, L. F., Song, C. L., Cao, X. Y., and Zhou, Y. Y. (2023). Metagenomic insights into feasibility of agricultural wastes on optimizing water quality and natural bait by regulating microbial loop. *Environ. Res.* 217:114941. doi: 10.1016/j.envres.2022.114941
- Wang, J. Z., Xue, L. H., Hou, P. F., Hao, T. J., Xue, L. X., Zhang, X., et al. (2023). Struvite as P fertilizer on yield, nutrient uptake and soil nutrient status in the rice-wheat rotation system: a two-year field observation. *Agronomy* 13:2948. doi: 10.3390/agronomy13122948
- Wang, Y., Mou, J., Liu, X., and Chang, J. (2021). Phosphorus recovery from wastewater by struvite in response to initial nutrients concentration and nitrogen/phosphorus molar ratio. *Sci. Total Environ.* 789:147970. doi: 10.1016/j.scitotenv.2021.147970
- Woodruff, D. P. (2016). "Methods of surface composition determination," in *Modern Techniques of Surface Science* (3rd ed.), ed. D. P. Woodruff (Cambridge: Cambridge University Press), 35–97.
- Yaakob, M. A., Mohamed, R. M., Al-Gheethi, A., Aswathnarayana Gokare, R., and Ambati, R. R. (2021). Influence of nitrogen and phosphorus on microalgal growth, biomass, lipid, and fatty acid production: an overview. *Cells* 10:393. doi: 10.3390/cells10020393
- Yang, H. R., Liu, Y., Hu, S. J., Zhang, M. Y., Wu, D., Zheng, L., et al. (2024). Advanced electrochemical membrane technologies for near-complete resource recovery and zero-discharge of urine: performance optimization and evaluation. *Water Res.* 263:122175. doi: 10.1016/j.watres.2024.122175
- Zeng, W. S., Wang, D. H., Wu, Z. Y., He, L. T., Luo, Z. F., and Yang, J. (2021). Recovery of nitrogen and phosphorus fertilizer from pig farm biogas slurry and incinerated chicken manure fly ash. *Sci. Total Environ.* 782:146856. doi: 10.1016/j.scitotenv.2021.146856
- Zhai, Q., Hong, Y., Wang, X., Wang, Q., Zhao, G., Liu, X., et al. (2022). Mixing starch wastewaters to balance nutrients for improving nutrient removal, microalgae growth and accumulation of high value-added products. *Water Cycle* 3, 151–159. doi: 10.1016/j.watcyc.2022.09.004
- Zhang, B., Tian, S. Y., and Wu, D. L. (2023). An integrated strategy for nutrient harvesting from hydrolyzed human urine as high-purity products: tracking of precipitation transformation and precise regulation. *Sci. Total Environ.* 854:158721. doi: 10.1016/j.scitotenv.2022.158721
- Zhang, D., Yang, H. L., Lan, S. H., Li, X. D., Guo, Q., and Xie, Y. F. (2023). An innovative bilayer solid carbon source for tertiary denitrification: synthesis, performance, and microbial diversity analysis. *J. Water Process Eng.* 54:103931. doi: 10.1016/j.jwpe.2023.103931
- Zhang, M., Wang, X., Zhang, D., Zhao, G., Zhou, B., Wang, D., et al. (2022). Food waste hydrolysate as a carbon source to improve nitrogen removal performance of high ammonium and high salt wastewater in a sequencing batch reactor. *Bioresour. Technol.* 349:126855. doi: 10.1016/j.biortech.2022.126855
- Zhang, S. J., Mao, Y. P., Sun, J., Song, T. L., Song, Z. L., Zhao, X. Q., et al. (2023). One-pot solvothermal preparation of triple-emission N, Cl doped carbon quantum dots from waste traditional Chinese medicines as a fluorescent sensor for sensing water and Cr (VI). *Colloids Surf. A* 669:131471. doi: 10.1016/j.colsurfa.2023.131471
- Zhang, T., He, X. Y., Deng, Y. X., Tsang, D. C. W., Yuan, H. M., Shen, J. B., et al. (2020). Swine manure valorization for phosphorus and nitrogen recovery by catalytic -thermal hydrolysis and struvite crystallization. *Sci. Total Environ.* 729:138999. doi: 10.1016/j.scitotenv.2020.138999
- Zhao, C., Peng, D. P., Huang, Z. J., Wu, Z., and Huang, T. (2024). Magnesium-modified starch cryogels for the recovery of nitrogen and phosphorus from wastewater and its potential as a fertilizer substitute: a novel nutrient recovery approach. *J. Environ. Chem. Eng.* 12:114044. doi: 10.1016/j.jece.2024.114044
- Zheng, M., Xie, T., Li, J., Xu, K., and Wang, C. (2018). Biochar as a carrier of struvite precipitation for nitrogen and phosphorus recovery from urine. *J. Environ. Eng.* 144:04018101. doi: 10.1061/(ASCE)EE.1943-7870.0001450
- Zheng, S., Xu, X., Chen, G., Zhou, J., Ma, F., and Du, C. (2023). Rapid detection of phosphorus in water using silicon attenuated total reflectance infrared spectroscopy coupled with the algorithms of deconvolution and partial least squares regression. *Sens. Actuators B Chem.* 380:133372. doi: 10.1016/j.snb.2023.133372
- Zhou, Y. G., Liu, Z. H., Shan, J. H., Wu, C. Y., Lichtfouse, E., and Liu, H. B. (2024). Efficient recovery of phosphate from urine using magnesite modified corn straw biochar and its potential application as fertilizer. *J. Environ. Chem. Eng.* 12:111925. doi: 10.1016/j.jece.2024.111925
- Zhu, D. C., Chen, Y. Q., Yang, H. P., Wang, S. H., Wang, X. H., Zhang, S. H., et al. (2020). Synthesis and characterization of magnesium oxide nanoparticle-containing biochar composites for efficient phosphorus removal from aqueous solution. *Chemosphere* 247:125847. doi: 10.1016/j.chemosphere.2020.125847
- Zin, M. M. T., and Kim, D. J. (2021). Simultaneous recovery of phosphorus and nitrogen from sewage sludge ash and food wastewater as struvite by Mg-biochar. *J. Hazard. Mater.* 403:123704. doi: 10.1016/j.jhazmat.2020.123704